Soot Track Formation by Shock Waves and Detonations

Kazuaki Inaba[1]**, Akiko Matsuo**[2]**, Joseph E. Shepherd**[3]
[1]Graduate school of Keio University, Yokohama, Kanagawa JAPAN
[2]Keio University, Yokohama, Kanagawa JAPAN
[3]Caltech, Pasadena, CA USA

Corresponding author, K. Inaba: harlock_kazz@1999.jukuin.keio.ac.jp

Introduction

For over 40 years, the soot track method has been widely used as an indication of detonation propagation and a semi-quantitative tool for measuring the cell size and classifying the regularity of the cellular structure (Fickette & Davis[1]). Although it is readily apparent that the soot tracks are associated with frontal shock waves and transverse waves, triple-point trajectories derived from PLIF of the OH radical near the soot foil do not agree with the soot tracks in a preliminary experiment by Pintgen & Shepherd [2]. Speculation on the mechanism has included pushing the soot with pressure gradients, "scrubbing" the soot off by vortices [3], and combustion of the soot in hot oxidizing atmospheres [4]. However, the precise physical mechanism that creates the soot tracks has never been clearly demonstrated. The removal process of fine (soot) particles from surface has wide applications for semiconductor industry and the conservation of works of art and historic building. The goal of the present study is to explore an explanation that is based on the classical fluid mechanics of near-wall flow in a viscous gas.

Fletcher [5] examined the interaction between a dusty layer of particles and passing shock waves related to coal mine explosions, and reported that dust was raised as a result of the rapid flow following behind the shock wave, rather than as that of a pressure wave passing through the dust layer. Although the dust rising may not be identical phenomena with the soot track formation, we start our discussion, based on Fletcher's observations. We propose that the soot tracks depend largely on variations in the direction and magnitude of the shear stress created by the boundary layer adjacent to the soot foil. Our proposal is motivated by three key observations: 1) soot tracks can be formed in Mach reflection of a non-reactive shock [6], 2) pattern formation in oil flow visualization can be completely explained in terms of surface shear stress [7], and 3) the process of Mach reflection in a non-reactive gas contains all the essential features of the shock configurations in detonation fronts. We performed numerical simulations of Mach reflection and the associated boundary layers in order to estimate the shear stress and pressure distribution that will affect a soot layer [8]. In this paper, simple models of soot motions will be simulated to interpret the influences of shear stress, treating the soot layer as clumps of fine particles and as incompressible fluid.

Numerical Setup

The flow behind the shock wave was investigated by numerically simulating the three-dimensional compressible Navier-Stokes equations. As a numerical scheme, Yee's non-MUSCL type TVD upwind explicit scheme [9] is utilized. Initial conditions are listed in Table 1. Here, θ_w is an apex angle of a wedge. As shown in Fig. 1, a stretched grid system is used and the number of grid points is $151 \times 101 \times 51$ ($185 \times 114 \times 5.6$ mm). We adopt a shock-fixed coordinate system; the bottom $x - z$ plane (a non-slip and isothermal boundary condition) corresponds to a soot foil and

Table 1: Initial conditions and soot-track/triple-point track angles. (exp., experiment; sim., simulation of gas phase; soot, simulation of soot; *maximum curvature point in vNR)

case	M_s	θ_w °	p_1/p_0	T_1/T_0	$Re \times 10^7$ m^{-1}	$\chi_{exp.}$ °	$\chi_{sim.}$ °	χ_{soot} °
A	1.9	15	4.05	1.61	4.27	16	17	15
B	1.9	25	4.05	1.61	4.27	10	12	9.0
C	1.2	15	1.51	1.13	2.70	7.8	11*	9.0
D	1.2	25	1.51	1.13	2.70	5.2	5.9*	5.3

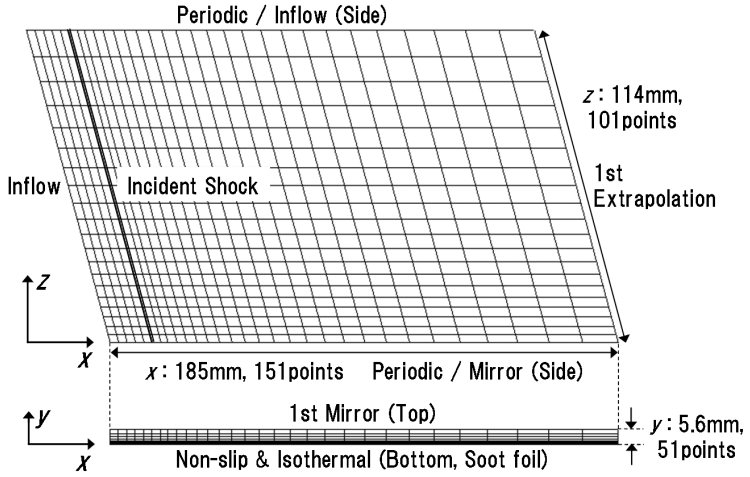

Figure 1: Computational grid and Boundary conditions.

is moving at the same speed as the shock. The modeling of soot motion are carried out with two aspects; the first is that the soot is treated as a continuum like thin oil film; the second is that the soot is regarded as aggregate of particles such as sediments in rivers.

a) Oil film model If the film is thin enough, the dominant force is the skin friction, and a simple relation is obtained between the film thickness variation and the skin friction distribution. Assuming that the soot is approximated as an incompressible fluid, the soot thickness h obeys the following conservation equation [10];

$$\frac{\partial h}{\partial t} = -\frac{\partial}{\partial x}\int_0^h u dy - \frac{\partial}{\partial z}\int_0^h w dy \tag{1}$$

Assuming the Couette flow for soot, velocity components of u and w become followings [7];

$$u = \frac{\tau_{yx} y}{\mu_s}, \quad w = \frac{\tau_{yz} y}{\mu_s} \tag{2}$$

where $u, w, \tau_{yx}, \tau_{yz}$ are the velocity components and the shear stresses arising from the gaseous boundary layer in x and z directions, respectively, and μ_s is viscosity coefficient of the soot layer. The governing equations (1, 2) are discretized with MacCormack scheme in the 2-D computational

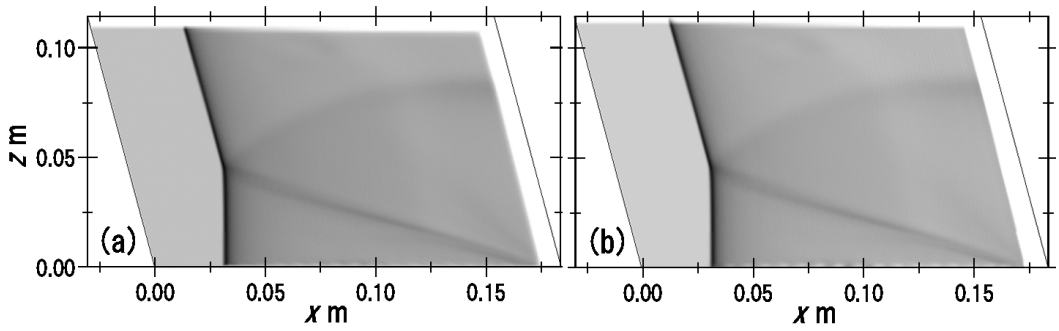

Figure 2: Soot thickness distributions in case A. (a) Oil film model. (b) Sliding particle model.

domain (301 × 101 grid points) that has the same cross-section area of 3-D grid for air. Shear stresses of air drive soot, though soot-thickness distributions do not affect air flow; hence, one-way coupling is assumed.

b) Sliding particle model The discrete particle approach is utilized for numerical simulations. Each of these particles characterizes a set of physical particles having the same characteristics such as location, velocity, radius, and mass. The particle is assumed to consist of spherical particles which distribute in the computational $x-z$ plane. The governing equations of soot particles become followings;

$$\frac{\mathrm{d}\mathbf{I}_i}{\mathrm{d}t} = \mathbf{F}_i, \quad \mathbf{I}_i = \begin{bmatrix} x_i \\ z_i \\ u_i \\ w_i \end{bmatrix}, \quad \mathbf{F}_i = \begin{bmatrix} u_i \\ w_i \\ \left(f_x/m_p\right)_i \\ \left(f_z/m_p\right)_i \end{bmatrix} \tag{3}$$

where $f_x = \pi r_p^2 \overline{\tau}_{yx}, f_x = \pi r_p^2 \overline{\tau}_{yz}$ are tractive forces for x, z-components, $m_p \left(= 4/3\pi r_p^3 \rho_s\right)$ and r_p are mass and radius of a soot particle, respectively, and ρ_s (= 1200 kg/m^3) is soot density. The governing equations (3) are solved by the fourth-order Runge-Kutta method. Initially, 64 particles are arranged in each computational cell (300 × 100 cells).

Results and Discussion

Simulations of soot thickness are performed, using shear stress histories of gas phase. Figure 2(a) shows the soot thickness h normalized by the initial soot thickness h_0 in case A with the oil film model in the form of gray-scale distribution. The shock front propagates from right to left. The darker color indicates the thicker region. In this model, parameters are initial soot thickness h_0 (= 5.0 mm) and soot viscosity. The soot viscosity is not well known and is approximated with the property of water $\mu_{water} = 8.9 \times 10^{-4}$ Pa s at 298.15 K. As the initial soot thickness decreases with μ_{water}, variation of soot thickness becomes flattened, and at last most of the soot just remains on the wall. Even if arbitrary viscosity coefficient is chosen (e.g. $\mu_{air} = 18.2 \times 10^{-6}$ Pa s), the same feature of soot tracks can be obtained with the initial soot thickness (h_0 = 0.1 mm for air, 1/50 for water). In Fig. 2(a), soot is piled up and forms soot tracks. Soot track angle χ_{soot} around the leading edge as vertex (the right bottom corner, x = 0.185 m, z = 0.0 m) is 15° in Table 1, and is comparatively close to the experimental track angle $\chi_{exp.}$. The soot track angles $\chi_{exp.}$ and

χ_{soot} are smaller than numerical trajectory angles of triple points $\chi_{sim.}$. The parameters adopted in the simulations for soot redistributions are regarded as adjusting parameters, and thus arbitrary angles of numerical soot tracks might be obtained. The whole angles, however, would become less than the angles of triple points because the soot behind the incident shock is redistributed, being transported downward. With the sliding particle model, a similar result to the oil film model is obtained as shown in Fig. 2(b). Parameters in this model are initial soot thickness h_0(= 20 μm) and particle radius r_p(= 0.27 nm). Initial soot thickness is not important for sharpness of soot tracks, but the particle radius dominates the magnitude of soot thickness variations. The radius of numerical particles is quite smaller than that of typical soot particle.

On soot foil records in detonations, the soot where the Mach stem propagates is usually darker than the portion where incident shock propagates. Some soot tracks of H_2-O_2-Ar mixture shows that the soot inside the Mach funnel is darker than that of incident shock side, and that the soot looks piled up inside the funnel. The soot piled up inside the trajectory of triple points seems to be pushed forward due to the effect of the post-shock flow. Although the mechanism in detonation might be explained with the same mechanism observed in Mach reflections, triple points in detonations produce extremely high-pressure and large pressure gradients. Studies of drag on a spherical particle subject to an impulsively started flow behind a shock wave (Igra & Takayama [11]), and detachment of a single 400 μm diameter particle from the wall of a shock tube (Suzuki *et al*. [12]) revealed that the drag coefficient was nearly twice that in an equivalent steady flow. As a future work, numerical simulations taking account of the force of impulsive pressure and triple points in detonations will be useful to understand the transport and removal of fine soot particles.

Summary

Soot track formations were investigated with simple models of soot layer in 2-D simulations with spatial and temporal distributions of shear stress obtained in 3-D simulations of Mach reflection flows over wedges. Soot track angles obtained in experiments and simulations were slightly smaller than numerical trajectory angles of triple points. It was suggested that the soot tracks were piled up below the triple point trajectories because of the soot behind the incident shock, being transported downward.

References

[1] W. Fickett & W. C. Davis, *Detonation*, University of California Press, Berkeley, (1979).
[2] F. Pintgen & J. E. Shepherd, *Proc. 19th ICDERS*, Hakone, Japan (2003).
[3] P. Krehl & M. van del Geest, *Shock Waves*, **1**, (1991), pp. 3-15.
[4] K. Terao & T. Azumatei, *Jpn. J. Appl. Phys.*, **28**, (1989), pp. 723-728.
[5] B. Fletcher, *J. Phys. D: Appl. Phys.*, **9**, (1976), pp. 197-202.
[6] A. K. W. Lam, J. M. Austin, F. Pintgen, E. Wintenberger, J. E. Shepherd, K. Inaba, A. Matsuo, *Proc. 19th ICDERS*, Hakone, Japan (2003).
[7] L. H. Tanner & L. G. Blows, *J. Phys. E; Sci. Inst.*, **9**, (1976), pp. 194-202.
[8] K. Inaba, A. Matsuo, K. Tanaka, A. K. W. Lam, F. Pintgen, E. Wintenberger, J. M. Austin, J. E. Shepherd, *Proc. 19th ICDERS*, Hakone, Japan (2003).
[9] H. C. Yee, *NASA TM* 89464, (1987).
[10] L. C. Squire, *AGARDograph*, **70**, (1962), pp. 7-28.
[11] O. Igra & K. Takayama, *Proc. R. Soc. Lond. A*, **442**, (1993), pp. 231-247.
[12] T. Suzuki, Y. Sakamura, T. Adachi, S. Kobayashi, *Trans. Japan Soc. Aero. Space Sci.*, **38**, (1995), pp. 243-250.